Piezometric response in shallow bedrock at CB1: Implications for runoff generation and landsliding

David R. Montgomery,[1] William E. Dietrich,[2] and John T. Heffner[3]

Received 6 May 2002; revised 3 June 2002; accepted 25 June 2002; published 6 December 2002.

[1] Experimental observations comparing two steep unchanneled valleys in the Oregon Coast Range, one intensively instrumented (CB1) and the other monitored for runoff but which produced a debris flow (CB2), shed light on the mechanisms of shallow flow in bedrock, its interaction with the vadose zone, and its role in generating landslides. Previous work at CB1 led to the proposal that during storms pulses of rainfall transmit pressure waves through the vadose zone and down to the saturated zone to create rapid pore pressure response and runoff [*Torres et al.*, 1998]. Here, we document the associated rapid pore pressure response in the shallow fractured bedrock that underlies these colluvium-mantled sites and examine its influence on the generation of storm flow, seasonal variations in base flow, and slope stability in the overlying colluvial soil. Our observations document rapid piezometric response in the shallow bedrock and a substantial contribution of shallow fracture flow to both storm flow and seasonal variations in base flow. Saturated hydraulic conductivity in the colluvial soil decreases with depth below the ground surface, but the conductivity of the near-surface bedrock displays no depth dependence and varies over five orders of magnitude. Analysis of runoff intensity and duration in a series of storms that did and did not trigger debris flows in the surrounding area shows that the landslide inducing storms had the greatest intensity over durations similar to those predicted by a simple model of piezometric response. During a monitored storm in February 1992, the channel head at the base of the neighboring CB2 site failed as a debris flow. Automated piezometric measurements document that the CB2 debris flow initiated several hours after peak discharge, coincident with localized development of upward spikes of pressure head from near-surface bedrock into the overlying colluvial soil in CB1. Artesian flow observed exfiltrating from bedrock fractures on the failure surfaces at CB2 further implicates bedrock fracture flow in both runoff generation by subsurface storm flow and suggests a connection to landslide initiation. Our observations show that the timing of shallow landslide initiation can be delayed relative to both peak rainfall and peak runoff and support the argument that the influence of fracture flow on shallow landsliding helps explain the wide variability in the occurrence of slope instability in topographically analogous locations. *INDEX TERMS:* 1860 Hydrology: Runoff and streamflow; 1815 Hydrology: Erosion and sedimentation; 1824 Hydrology: Geomorphology (1625); *KEYWORDS:* runoff, landsliding

Citation: Montgomery, D. R., W. E. Dietrich, and J. T. Heffner, Piezometric response in shallow bedrock at CB1: Implications for runoff generation and landsliding, *Water Resour. Res.*, *38*(12), 1274, doi:10.1029/2002WR001429, 2002.

1. Introduction

[2] Topographically controlled convergence of subsurface flow makes hillslope hollows a focus of recurrent landsliding in steep soil-mantled terrain [e.g., *Dietrich and Dunne*, 1978; *Dietrich et al.*, 1986]. Topographically driven hydrologic models therefore provide a framework for interpreting field observations that shallow landslides typically occur on steep convergent slopes [*Reneau and Dietrich*, 1987; *Ellen et al.*, 1988] and especially at channel heads [*Montgomery and Dietrich*, 1988]. Models of shallow landslide initiation generally assume that slope failure occurs at a critical pore pressure or relative soil profile saturation and the advent of geographical information system (GIS) technology has spawned methods for combining hydrologic and slope stability models to predict locations susceptible to debris-flow initiation and runout using digital topography [*Okimura and Ichikawa*, 1985; *Okimura and Nakagawa*, 1988; *Dietrich et al.*, 1993, 1995, 2001; *Ellen et al.*, 1993; *Montgomery and Dietrich*, 1994; *Wu and Sidle*, 1995; *Burton and Bathurst*, 1998; *Montgomery et al.*, 1998, 2000, 2001]. In most coupled hydrologic-slope stability models, subsurface storm flow is treated as developing on

[1] Department of Earth and Space Sciences, University of Washington, Seattle, Washington, USA.
[2] Department of Earth and Planetary Science, University of California, Berkeley, California, USA.
[3] Environmental Research, Weyerhaeuser Company, Centralia, Washington, USA.

0043-1397/02/2002WR001429$09.00

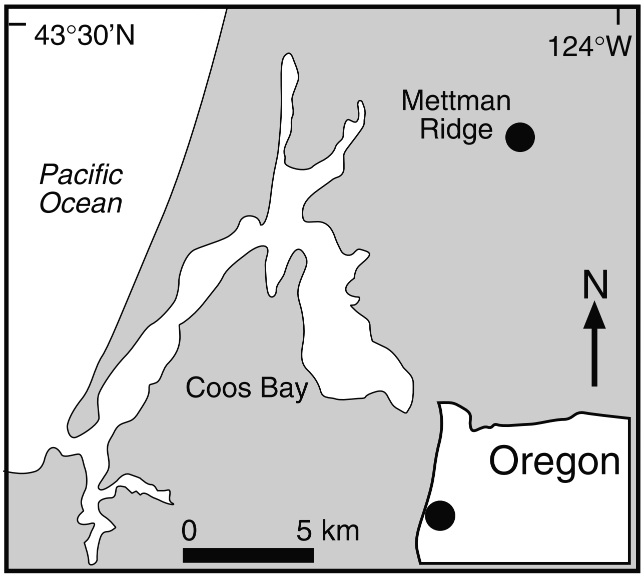

Figure 1. Location map for the Mettman Ridge study area near Coos Bay, Oregon.

a subsurface impeding layer (typically assumed to be the soil–bedrock boundary). This flow is assumed to travel downslope following surface topography. Several workers, however, have suggested a significant role of shallow fracture flow on landslide initiation [*Pierson*, 1977; *Everett*, 1979; *Wilson and Dietrich*, 1987; *Mathewson et al.*, 1990; *Montgomery et al.*, 1997]. A substantial influence of shallow fracture flow on the piezometric response of colluvial soils and on debris flow initiation would help to explain: (1) shallow landslides that occur on planar and convex hillslopes [*Reneau and Dietrich*, 1987; *Ellen et al.*, 1988]; (2) differences in the timing and occurrence of landslides in topographically similar locations; and (3) variations in the frequency and location of landslides with bedrock type. Here we document event and seasonal dynamics of near-surface bedrock fracture flow at an experimental catchment, demonstrate the importance of shallow bedrock flow in both storm runoff and base flow generation, and present evidence for an influence on debris-flow initiation.

2. Study Site and Previous Experiments

[3] The study area is located on Mettman Ridge roughly 15 km north of Coos Bay, Oregon (Figure 1). The Mettman Ridge area consists of steep, highly dissected soil-mantled hillslopes and steep channels typical of the Oregon Coast Range. Landslides are a major geomorphic process in the Coast Range where hillslope hollows undergo a cycle of slow colluvium accumulation and periodic landsliding [e.g., *Dietrich and Dunne*, 1978; *Dietrich et al.*, 1986]. Many channels begin at small landslide scars [*Montgomery and Dietrich*, 1988] and the lower part of hollows may fail more frequently than the upper portions [*Dunne*, 1991]. Highly conductive soils overlying shallow bedrock on steep slopes of the Oregon Coast Range produce rapid increases in pore pressure in topographic hollows during storms [*Harr*, 1977; *Pierson*, 1980; *Montgomery et al.*, 1997]. Intensive timber harvesting and road construction throughout the range have dramatically increased rates of landsliding and sediment delivery to downstream channels [*Fredriksen*, 1970; *Brown and Krygier*, 1971; *Beschta*, 1978; *May*, 1998; *Montgomery et al.*, 2000].

[4] We instrumented two unchanneled valleys along Mettman Ridge (Figure 2). The CB1 catchment is a 51 m long, 860 m^2 unchanneled valley with an average slope of 43°. The CB2 catchment is a 3270 m^2 unchanneled valley with an average slope of 40°. Both study sites are underlain by relatively flat-lying Eocene sandstone [*Beaulieu and Hughes*, 1975] that produces stoney sandy soils. The cedar-hemlock forest native to the study area was clear-cut in 1987 and replanted with Douglas fir in 1988. Annual rainfall averages about 1500 mm, falling mostly during the winter wet season. The near-surface bedrock is variably fractured and weathered, and thin soils on topographic noses generally increase to 1.4–2.0 m thick along the hollows [*Montgomery et al.*, 1997] but with considerable local variability in soil thickness due to tree throw and animal burrows [*Schmidt*, 1999; *Heimsath et al.*, 2001]. Soil properties are typical of those reported for Coast Range soils developed on sandstone [e.g., *Harr and Yee*, 1975; *Schroeder and Alto*, 1983]. A weir installed at the base of CB2 monitored runoff from December 1989 until February 1992 when it was destroyed by a debris flow.

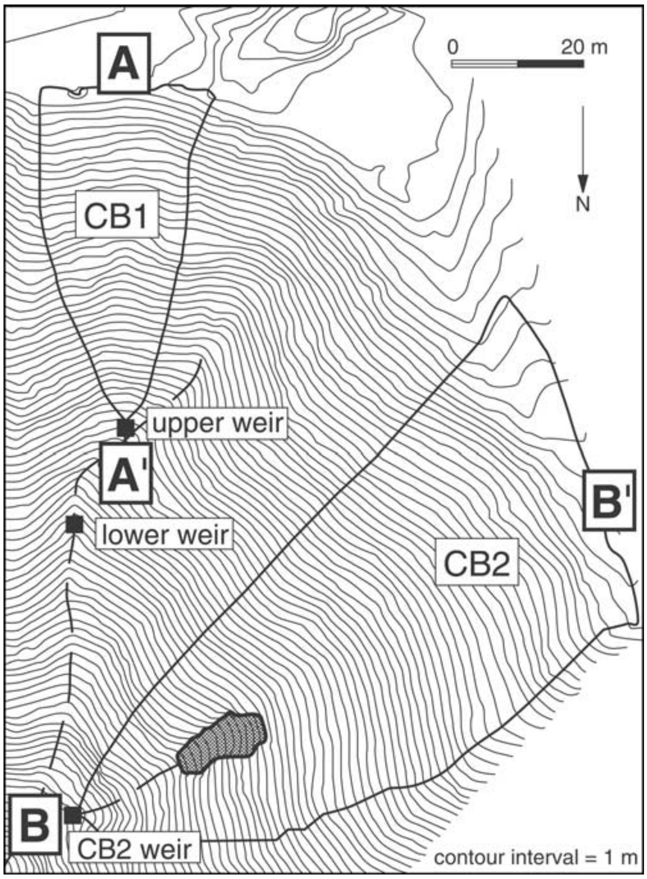

Figure 2. Map of the CB1 and CB2 catchments on Mettman Ridge; solid squares indicate the upper and lower CB1 weirs, and the CB2 weir. A–A′ indicates location of profile shown in Figure 4; B–B′ indicates location of profile shown in Figure 13. Small squares represent location of weirs. Shaded pattern in CB2 represents 1992 landslide scarp.

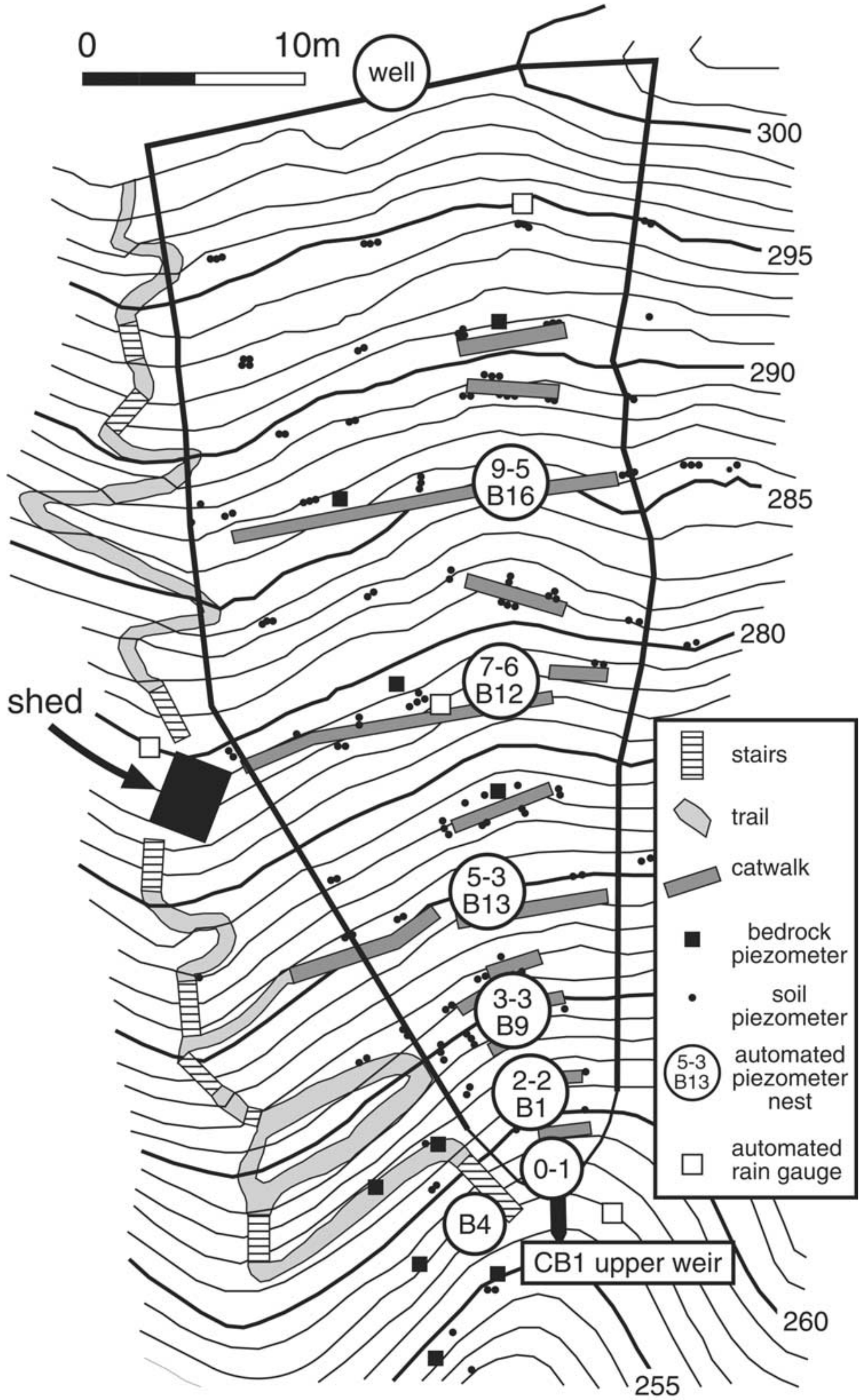

Figure 3. Map of CB1 showing location of bedrock piezometers; automated piezometer nests shown as open circles, other bedrock piezometers shown as black squares, and soil piezometers as small solid circles. Also shown are the catwalks, stairs and trails constructed at the site, as well as the location of automated rain gauges (open squares) and the upper CB1 weir. Contour interval = 1 m.

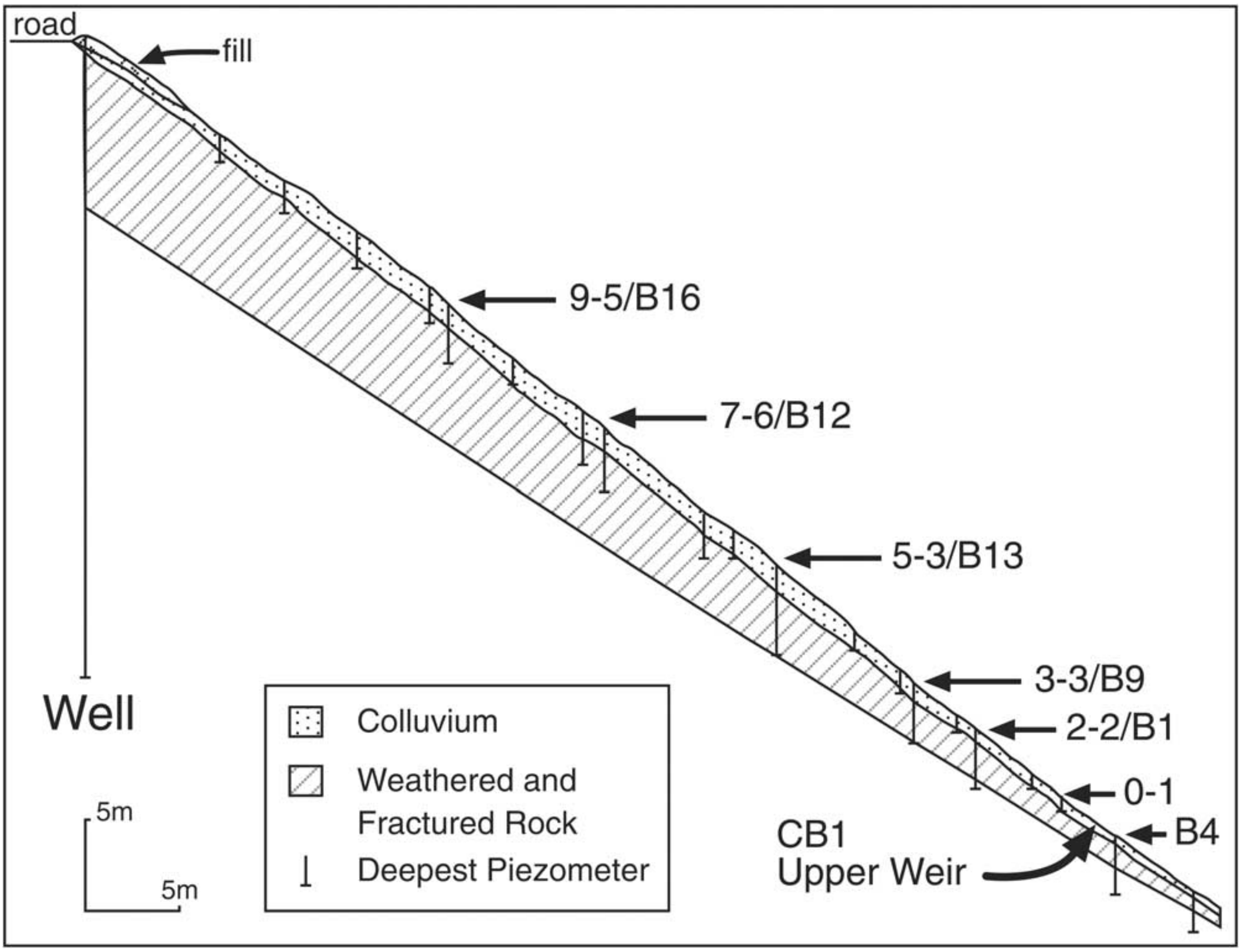

Figure 4. Long profile down CB1 showing location of piezometer nests referred to in text. Profile corresponds to A–A′ on Figure 2.

[5] An extensive piezometer array was installed at CB1 prior to a series of applied rainfall experiments in 1990 [*Montgomery et al.*, 1997, Experiments 1 and 2], and expanded to include a denser array in the soil, piezometers installed into bedrock, and a 35 m deep well on the ridge crest prior to subsequent experiments in 1992 (Figures 3 and 4). Piezometers were installed in 50.8-mm (2 inch) diameter borings and constructed of 25.4-mm (1 inch) diameter PVC pipe, of which the bottom 0.1 m was slotted using a hacksaw. Piezometers were installed on a thin (i.e., <0.01 m thick) bed of sand which was also used to backfill around the slotted section of pipe. A bentonite cap was emplaced on top of the sand and native material was used to backfill the rest of each boring. For the 10^{-3} to 10^{-4} m s^{-1} hydraulic conductivity of the colluvial soil at Mettman Ridge [*Montgomery et al.*, 1997], *Hvorslev*'s [1951] analysis indicates that the lag time required for piezometers to achieve 90% response to a change in pressure head is less than the 10 to 20 minute logging interval recorded by data loggers for the automated piezometers.

[6] Weirs installed at the base of CB1 and along the downslope colluvial channel monitored runoff from December 1989 until November 1996, when they too were destroyed by a debris flow. Additional details of the experiments, including artificial rainfall application and discussion of the results of tracer and tensiometer studies are presented elsewhere [*Anderson et al.*, 1997; *Montgomery et al.*, 1997; *Torres et al.*, 1998]. This paper presents the first analysis of saturated pore pressure response to a third applied rainfall experiment conducted in 1992.

2.1. Experiments 1 and 2

[7] Observations from these experiments and natural storms document that runoff generation occurs by subsurface storm flow. The sprinkling experiments showed that steady state runoff began from CB1 after piezometric potential reached steady state throughout the soil profile and that a steep soil moisture–pressure head relation allows the soil to transmit rapid pressure changes from pulses of rainfall at the ground surface through the unsaturated soil profile [*Torres et al.*, 1998], even though the applied water moves as vertical piston-like unsaturated flow [*Anderson et al.*, 1997]. During typical rainfall events, matric potential throughout the soil profile approaches zero [*Torres et al.*, 1998] and a narrow, discontinuous zone of positive pore pressure develops at the base of the soil profile along the hollow axis [*Montgomery et al.*, 1997], with a small area near the channel head delivering runoff to the upper CB1 weir [*Anderson et al.*, 1997; *Montgomery et al.*, 1997]. Exfiltrating head gradients develop locally from the bedrock into the colluvial soil in response to intense rainfall and the

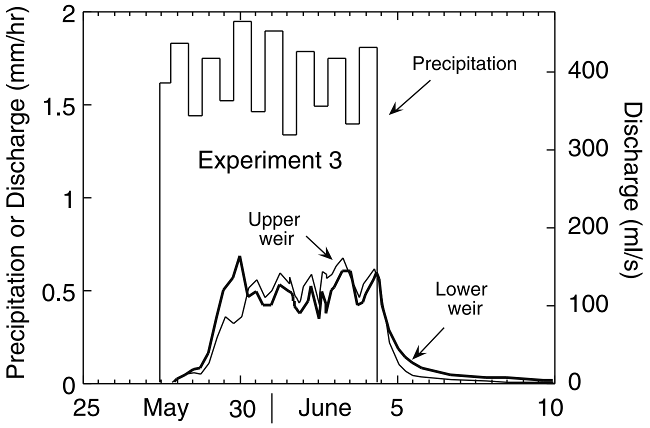

Figure 5. Precipitation and runoff during Experiment 3 from the upper CB1 weir (DW1) and the lower CB1 weir, lcoated along the downslope colluvial channel.

discontinuous zone of saturation during the steady state runoff of Experiments 1 and 2 was interpreted to reflect an interplay between flow in the colluvial soil and underlying fractured bedrock [*Montgomery et al.*, 1997]. Installation of piezometers drilled into the bedrock at CB1 after the 1990 experiments allowed us to examine near-surface bedrock response in subsequent experiments and natural rainfall.

3. Experiment 3

[8] Experiment 3 essentially repeated the steady, low-intensity precipitation applied during Experiment 1 [see *Montgomery et al.*, 1997], with an applied precipitation intensity of 1.65 ± 0.20 mm hr^{-1} sustained from 1000 h UT on 27 May through 0815 h UT on 3 June 1992. Dirunal fluctuations in discharge and pore pressure response during steady precipitation reflect variations both in evapotranspiration and in applied precipitation delivery due to daily variations in wind speed. During Experiment 3, runoff from the upper CB1 weir collected discharge from the colluvial soil that emerged at the channel head. Discharge that passed through the upper weir was routed around the lower weir. Hence, during the applied precipitation experiment the lower CB1 weir collected only water that flowed through the fractured bedrock beneath the upper CB1 weir and emerged downhill as spring flow. The total runoff through the two CB1 weirs during Experiment 3 accounted for 1.06 ± 0.15 mm hr^{-1}, 64% of the applied precipitation rate. Each of the CB1 weirs accounted for approximately a third of the applied precipitation rate (Figure 5). At this low-intensity rate of applied precipitation approximately half of the net runoff from CB1 follows a bedrock flowpath and emerges as spring discharge below the upper weir, with the remaining third of the applied precipitation accounted for by evapotranspiration and recharge of the local bedrock groundwater table.

[9] The pattern of saturation in the colluvial soil was nearly identical to that observed in response to the similar applied rainfall intensity of Experiment 1 (Figure 6). As in Experiment 1 [*Montgomery et al.*, 1997], four separate patches of saturated response developed in the colluvial soil during Experiment 3, and one of these areas was downslope and outside of the weir wings (which were sealed to bedrock). Hence, the expanded number of soil piezometers used in Experiment 3 document that the spatial gaps in response in the colluvial soil observed in Experiments 1 and 2 arose from a discontinuous pattern of saturation along the hollow axis, rather than from gaps in the original piezometer coverage. In contrast to the discontinuous saturation in the colluvial soil, the bedrock piezometers show a more continuous pattern. As for the soil response, the zone of bedrock response appears to be restricted to along the hollow axis. Hence, a perched water table that forms within the fractured bedrock locally supports a discontinuous saturated zone within the overlying colluvial soil. These observations, combined with tracer and solute monitoring [*Anderson et al.*, 1997], indicate that nearly all the runoff from CB1 passes through the bedrock before emerging from the soil at the upper CB1 weir or directly out of the bedrock between the upper and lower weirs.

[10] We conducted falling head conductivity tests on all piezometers at CB1 during steady state response in the second half of Experiment 3 when most tensiometers on site read close to zero pressure head [*Torres et al.*, 1998]. Tests were conducted by filling piezometers with water and measuring the rate of drawdown with a pressure transducer that recorded water level every 5 s, or by hand for slow draining piezometers. Saturated conductivity varies widely, but there are significant differences in the trends with depth for soil and bedrock piezometers (Figure 7). The hydraulic conductivity values for soil piezometers display an inverse correlation with piezometer inlet depth, varying from 10^{-3} to 10^{-4} m s^{-1} in shallow pipes to about 10^{-6} m s^{-1} in the deepest piezometers, with a mean value of 10^{-4} m s^{-1}. In contrast, bedrock and saprolite conductivities have a slightly lower mean value (4.7×10^{-5} m s^{-1}), but exhibit no relation to depth over five orders of magnitude (10^{-3} to 10^{-8} m s^{-1}). There is substantial variability in hydraulic conductivity at CB1, with roughly 2 orders-of-magnitude variation for piezometers at equal depth in the soil profile, and almost 5 orders-of-magnitude variability for bedrock piezometers installed at the same depth. Hence, there are strong contrasts in the variability and trend of hydraulic conductivity between the colluvial soil and near-surface bedrock: conductivity of the colluvial soil systematically decreases with depth, whereas the conductivity of the near surface bedrock is much more variable and is not systematically related to depth below the ground surface (Table 1). Moreover, the soil and bedrock conductivity distributions exhibit the opposite skewness (Figure 8). The right skewed distribution of soil conductivity implies that the colluvial soil is highly conductive in general with a few zones of low conductivity, whereas the left skewed distribution of bedrock conductivity indicates that the bedrock is poorly conductive in general with a few zones of high conductivity. Consequently, we would expect to find large spatial variability in the bedrock flow component of near surface hydrologic response with substantial flow concentration in a few areas of high conductivity.

[11] Patterns of bedrock piezometer response during Experiment 3 indicate that a variety of gradients across the bedrock/colluvium contact characterized places where saturated zones developed in the colluvial soil. For example, the response of the piezometer nest at the upper CB1 weir (see Figure 3a for location of piezometer nests) indicates

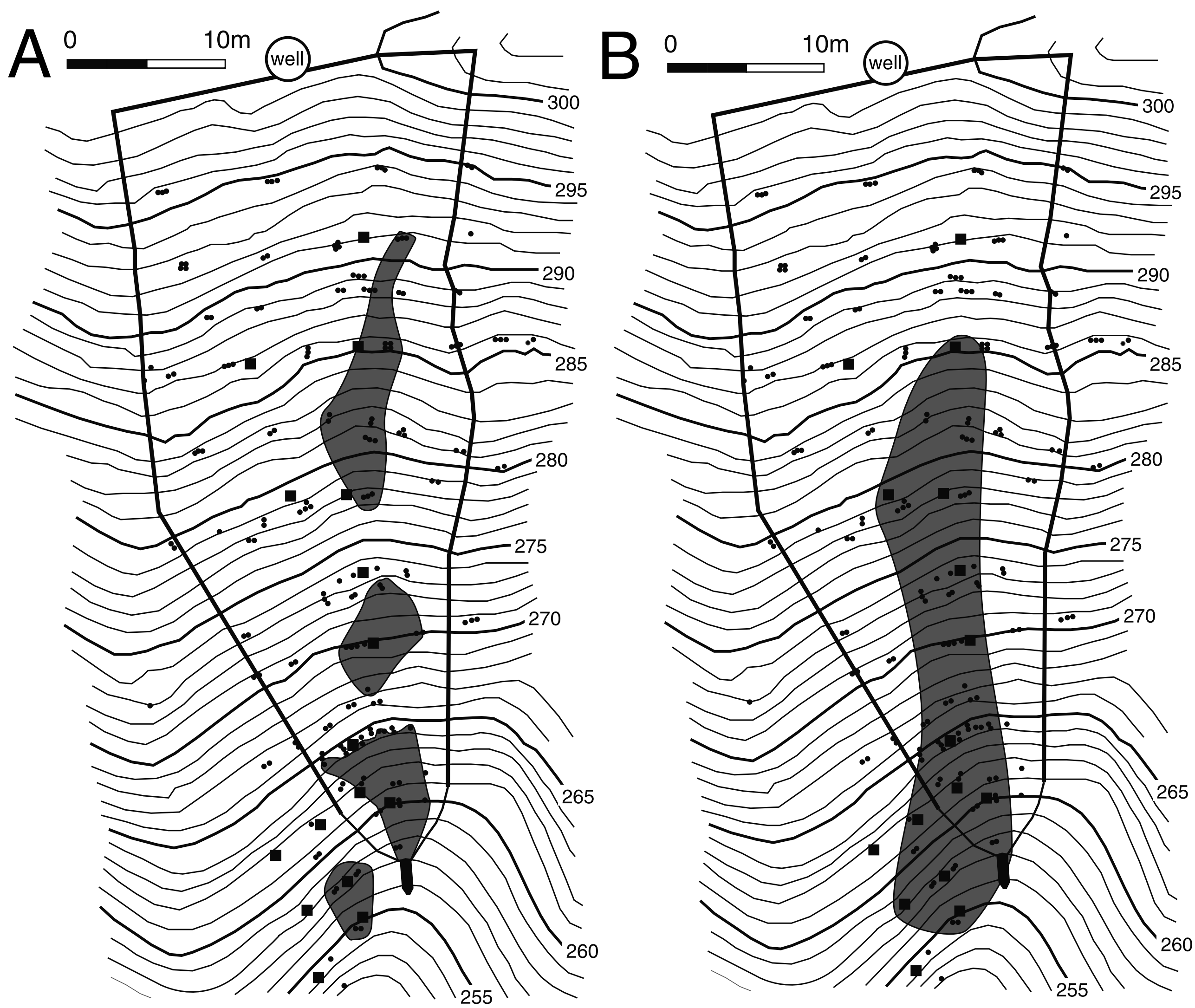

Figure 6. Zones of positive pore pressure response recorded in both manual and automated piezometers installed into (A) colluvial soil and (B) bedrock. North is to the bottom of the figure.

development of both a perched zone of saturation just above the colluvium–bedrock contact and deeper flow in the fractured bedrock (Figure 9a). The perched nature of the saturation in the colluvial soil is apparent in the response of piezometer nest 0-1 which shows substantial response even though the shallowest bedrock piezometer remained dry. The response of soil nest 5-3 and bedrock nest B-13 (3 m deeper) indicate slight exfiltrating gradients developed from the fractured rock into the soil until a bromide injection test [*Anderson et al.*, 1997] in the middle of the experiment interrupted the signal. In contrast, the response at soil nest 7-6 and bedrock nest B-12 show consistent infiltrating gradients throughout the experiment (Figure 9c). These different styles of response document the styles of soil–bedrock flow coupling inferred from the response of soil piezometers in Experiment 1 [*Montgomery et al.*, 1997]. In addition, even though flow through the sprinklers was held at a constant application rate, most of the piezometers displayed diurnal pore pressure oscillations driven by variations both in evapotranspiration and in precipitation delivery to the site due to the daily rise of afternoon winds. Hence, observations from Experiment 3 document that the piezometric response to even low-intensity rainfall can extend well beyond the penetration depth of the applied rainfall, as strong piezometric response was recorded in piezometers installed meters into bedrock even though a tracer included in the applied rainfall advanced only 0.2–0.3 m after its introduction during Experiment 3 [*Anderson et al.*, 1997].

[12] In addition, the deep well at the head of CB1 (Figure 2) exhibited a delayed but pronounced response to Experiment 3 (Figure 10). Prior to the start of Experiment 3, and during the first several days of the experiment, the water level in the well fell at a rate of 0.06 m day^{-1}. On 1 June, however, the water level in the well began to rise, continued to rise throughout the experiment, and then began to fall again one to two days after the sprinklers were turned off. The 3 to 4 day lag before the onset of irrigation was recorded at the water table 19.5 m below the ground surface implies that the signal propagated downward at a rate of about 5.6×10^{-5} m s^{-1} to 7.5×10^{-5} m s^{-1}. The response of the deep well shows that piezometric response at CB1 extended far beyond the depth to which the applied rainfall penetrated over the course of our experiments and that the

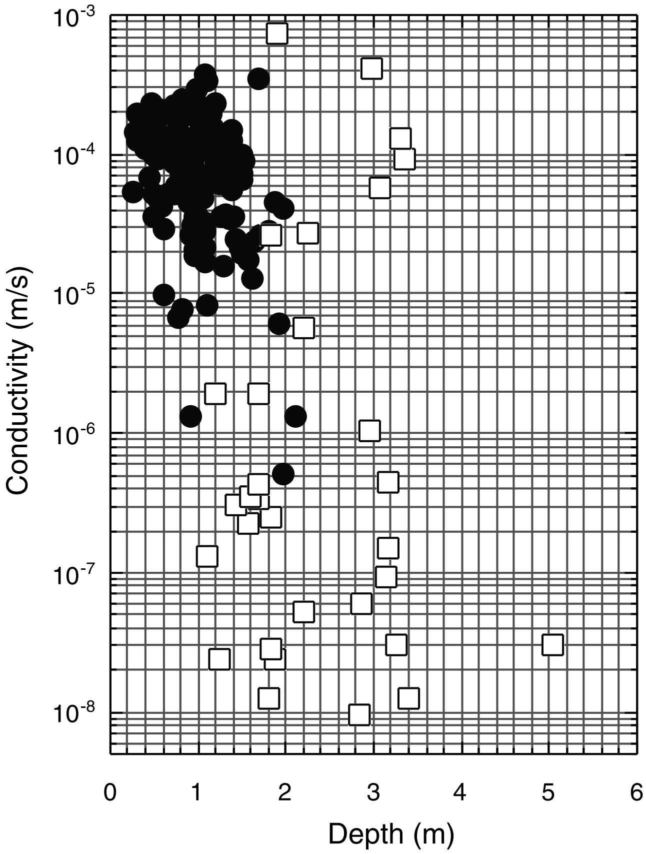

Figure 7. Hydraulic conductivity calculated from falling head test data versus depth of piezometer inlet for all piezometers installed in CB1. Solid circles are values from colluvial soil; open squares are values from saprolite and fractured bedrock.

pressure head signal propagated downward at close to the mean saturated hydraulic conductivity of the bedrock.

4. February 1992 Storm

[13] During a natural storm in February 1992 the channel head at CB2 failed as a debris flow. Although our piezometric data are from CB1, the two sites (CB1 and CB2) have similar runoff recession constants and runoff generation mechanisms [*Montgomery and Dietrich*, 2002]. Moreover, discharge recession constants for CB1 and CB2 during the February 1992 storm were typical for storms during this period, implying similar runoff generation mechanisms during the debris flow-producing event as for other monitored storms. Thus, we can reasonably extrapolate general insight from CB1 to CB2 in regard to relations among piezometric response and runoff generation, and thereby to hydrologic controls on debris-flow initiation.

[14] The failure of the area immediately above the channel head at CB2 on 20 February 1992, provides evidence for a link between near-surface flow in fractured bedrock and debris flow initiation. One of our colleagues (S. P. Anderson, personal communication, 1992) sampled the discharge through the CB2 weir at 10 am and discovered the landslide

Table 1. Distribution Characteristics for Saturated Hydraulic Conductivity Data for the CB1 Site

	Soil	Bedrock
Minimum, m s^{-1}	5.2×10^{-7}	9.4×10^{-9}
Maximum, m s^{-1}	3.7×10^{-4}	7.4×10^{-4}
Observations	135	32
Mean, m s^{-1}	1.0×10^{-4}	4.7×10^{-5}
Median, m s^{-1}	8.6×10^{-5}	3.2×10^{-7}
Std Deviation	7.6×10^{-5}	1.5×10^{-4}
Std Error	6.6×10^{-6}	2.6×10^{-5}

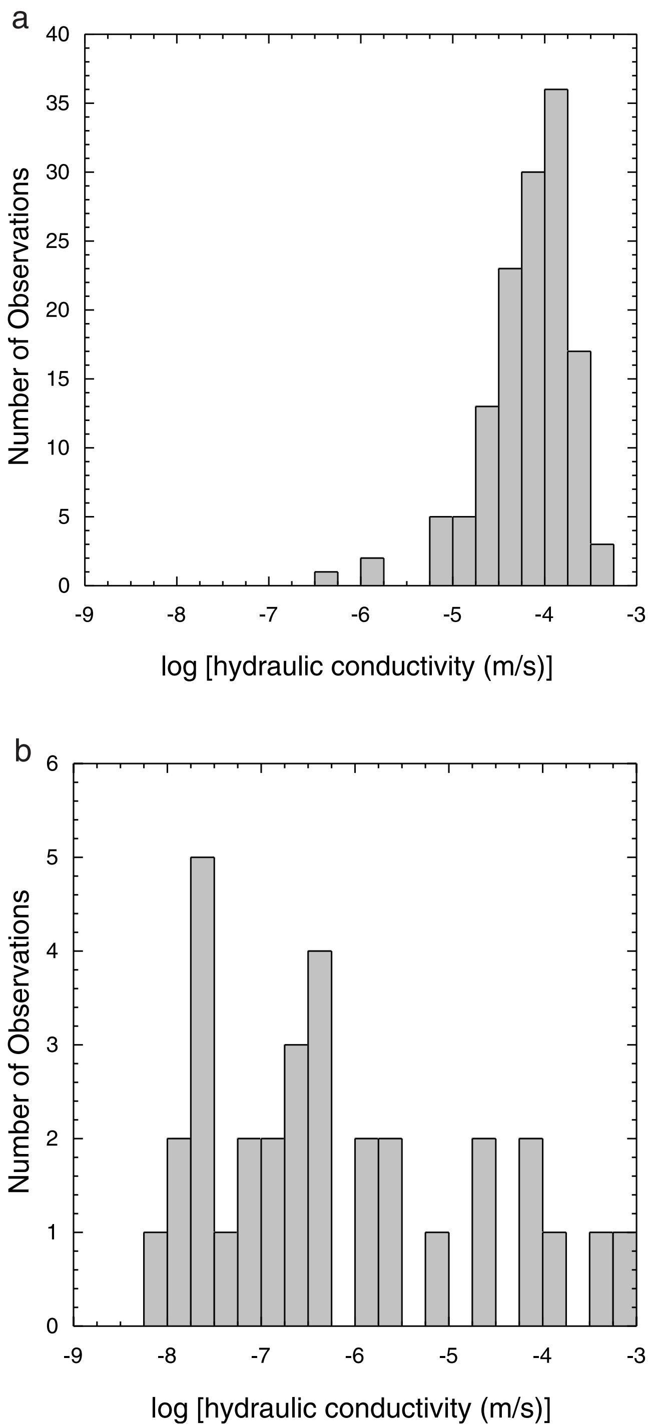

Figure 8. Frequency distributions of saturated hydraulic conductivity values from measurements of piezometers installed into (A) soil and (B) bedrock and saprolite.

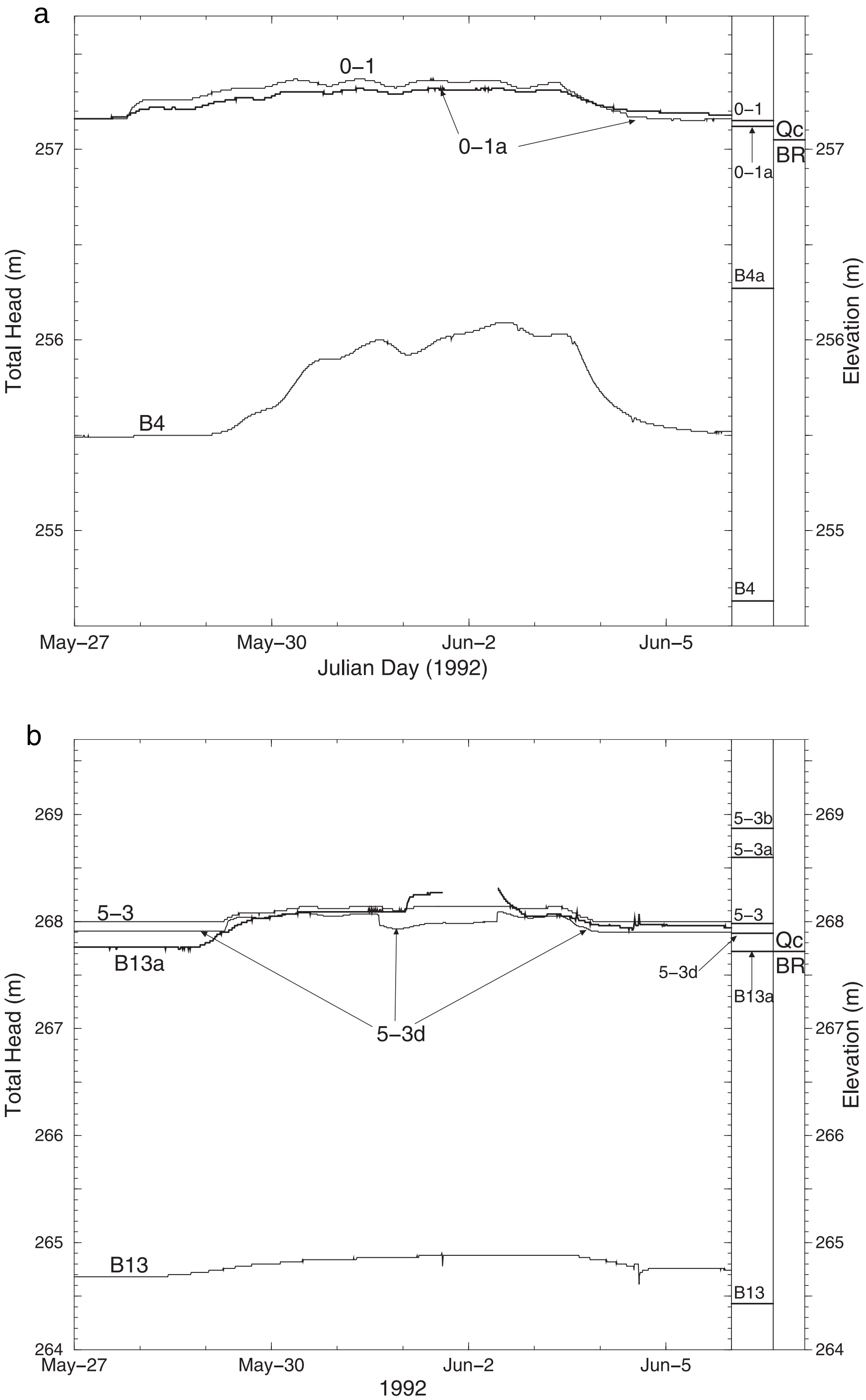

Figure 9. Piezometric response of three piezometer nests with pipes installed into near-surface bedrock during Experiment 3: (A) soil nest 0-1 and bedrock nest B4; (B) soil nest 5-3 and bedrock nest B13; and (C) soil nest 7-6 and bedrock nest B12. First vertical column on right of figure shows elevation of piezometer inlets and the second shows the elevation of the contact between colluvial soil (Qc) and bedrock (BR). Ground surface elevation corresponds to top of each graph.

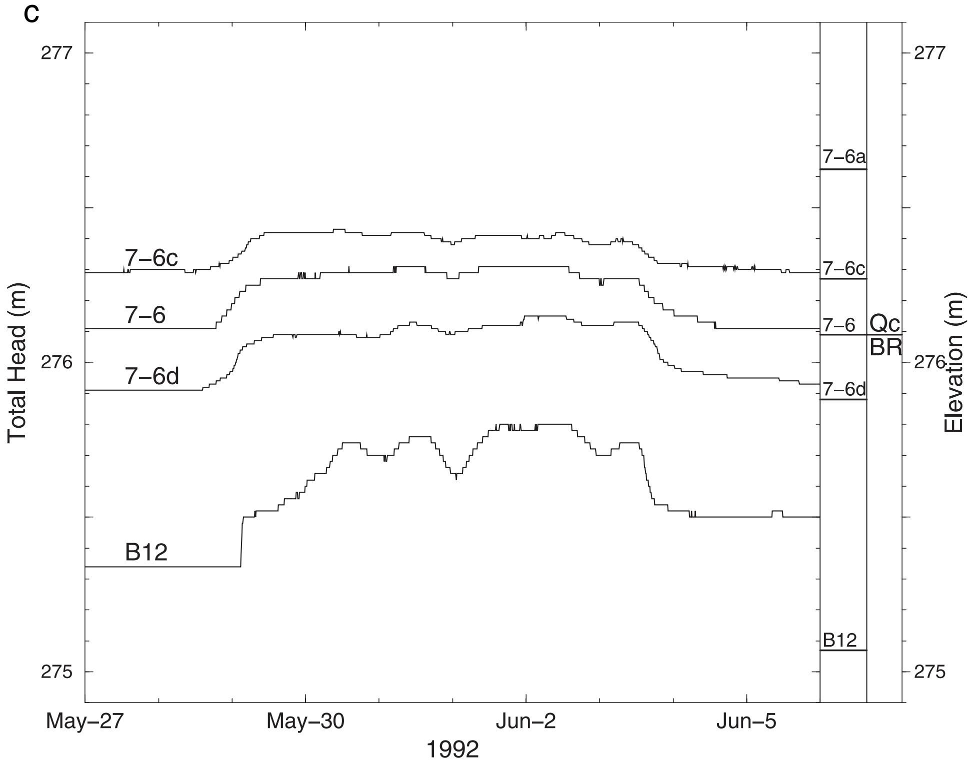

Figure 9. (continued)

upon returning at 1540 h UT. The resulting debris flow traversed the steep first-order bedrock channel through a high-angle tributary junction, and deposited behind an accumulation of logs incorporated in the deposits of previous debris flows. The data logger was intact and running when recovered from the deposit the following morning, documenting both when and at what stage the debris flow mobilized.

[15] The February 1992 storm was the largest event since continuous monitoring of the site began in late 1989. The landslide-inducing storm commenced with a series of low-intensity rainfall pulses that culminated in a peak intensity of 15.5 mm hr^{-1} at 7 am on 20 February and ended abruptly thereafter (Figure 11). The peak discharge of 3.9 l s^{-1} was sustained from 1000 to 1130 h UT, from 3 to 4.5 hours after peak rainfall. Slope failure, as recorded by termination of the CB2 discharge record, occurred at 1330 h UT, 2 to 3.5 hrs after the peak discharge (6.5 hours after peak rainfall) and at a discharge that the site experienced twice before in the 3 years of discharge data from CB2. This delay between peak discharge and slope failure could reflect either a time delay between peak runoff and peak pore pressure development, or a time-dependent transition of an initial transla-

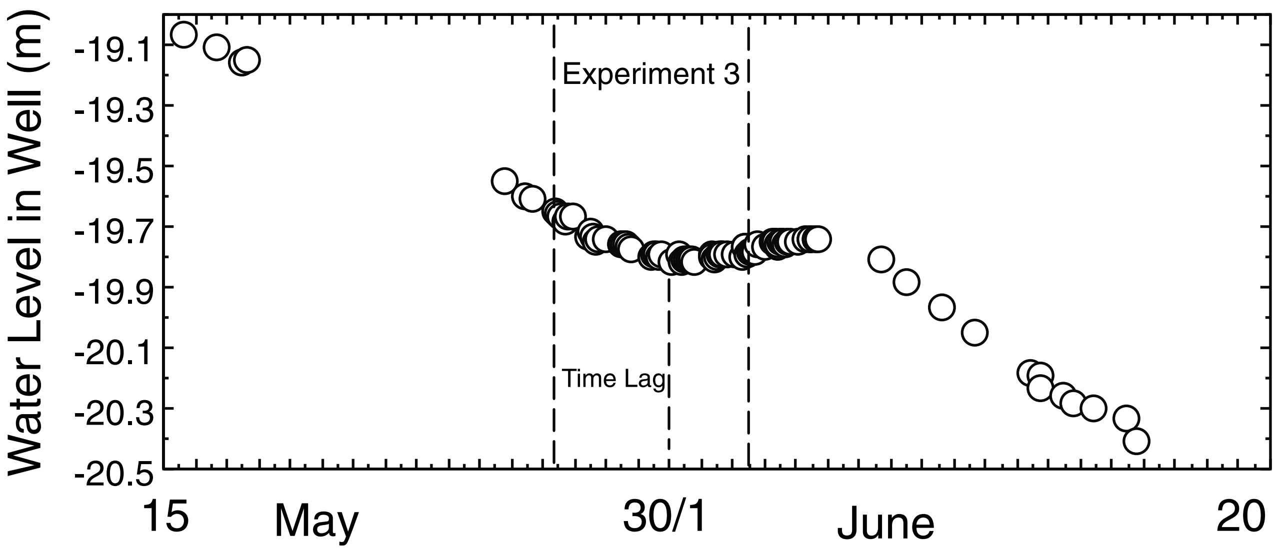

Figure 10. Response of the well located at the top of CB1 to applied rainfall during Experiment 3, expressed as the height of the water table below the ground surface.

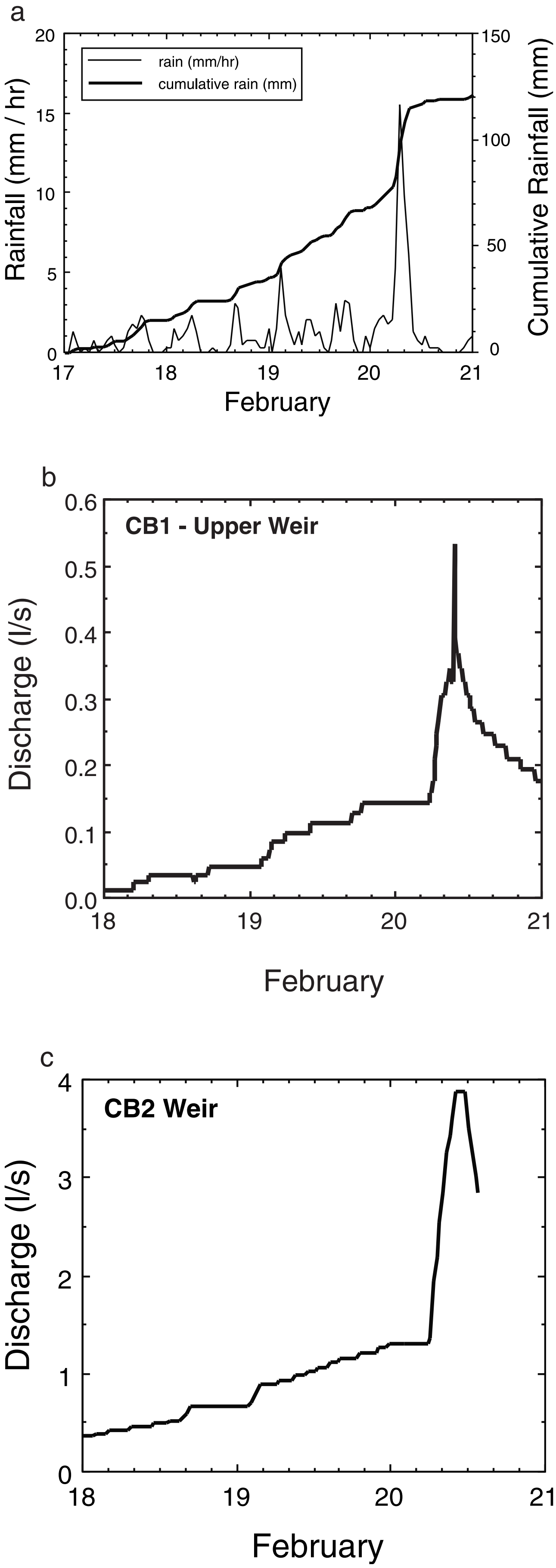

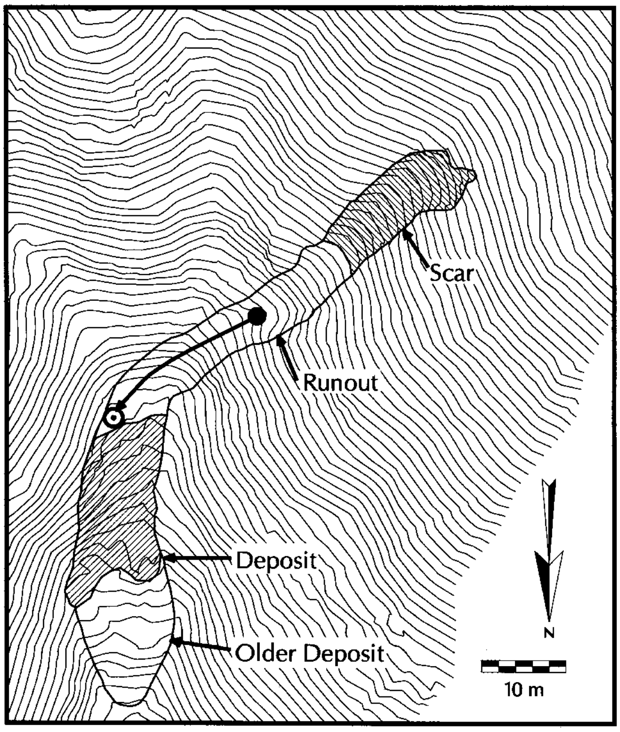

Figure 12. Topographic map of the 1992 CB2 landslide based on field surveys conducted with a total station digital theodolite. Contour interaval is 1 m. Arrow from closed circle to open circle connects initial location of CB2 weir and data logger to location in which the data logger was recovered after the 1992 debris flow.

tional failure into a debris flow. The 24-hr rainfall on 20 February was 53 mm and a total of 121 mm of rain fell during the four day storm sequence. Rainfall of 53 mm day^{-1} has an approximately 1-year recurrence interval based on comparison with long-term rain gauge records at North Bend, Oregon. Hence, even though the storm that caused failure of the channel head at CB2 was the largest in the 3 year record, it was not an extraordinary event.

4.1. CB2 Debris Flow

[16] The colluvium upslope of the CB2 channel head failed to bedrock, leaving a scar 1 m deep, 6.5 m wide, and 15 m long. Tension cracks extending laterally outward into the unfailed slope on either side of the headscarp indicate the initial movement of a larger volume of colluvium than mobilized as the debris flow. When first examined about 2 hours after failure, the headscarp hosted a seepage face and water gushed from bedrock fractures exposed at the base of the scar (S.P. Anderson, personal communication). The debris flow initially traveled straight downslope and then deposited along a steep (25°) channel after traversing an approximately 50° planform tributary junction (Figure 12).

Figure 11. (opposite) (A) Hourly and cumulative rainfall for 17 through 21 February 1992, recorded at CB1. (B) Discharge record for the CB1 upper weir for 17 through 21 February 1992. (C) Discharge record for CB2 for 17 through 21 February 1992. Termination of the discharge record records initiation of the CB2 debris flow.

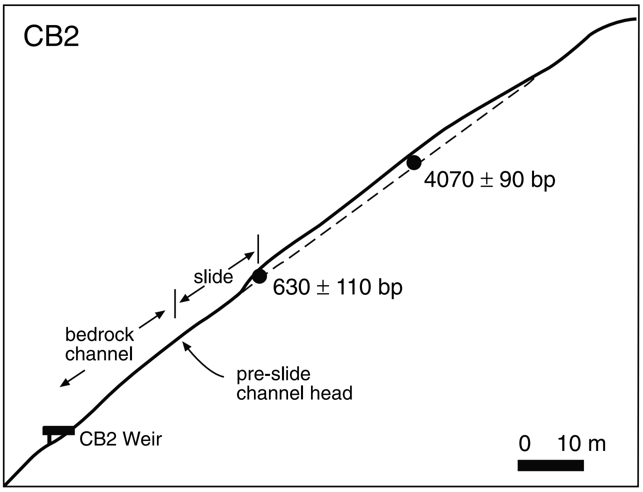

Figure 13. Surveyed longitudinal profile of CB2 showing location of samples collected for ^{14}C dating of detrital charcoal and the location of the CB2 weir. Profile runs from B to B′ on Figure 2.

[17] A series of cross-sections surveyed on the day after the debris flow using a hand level, stadia rod and fiberglass tape reveals that the debris flow traveled rapidly once mobilized. The edge of the debris-flow path was plainly demarcated by mud, debris and disturbed vegetation. The outer side of the debris flow elevated as it rounded the tributary confluence, allowing estimation of its mean velocity from the elevation difference between the flow surface on the inside and outside of the bend following the method discussed by *Costa* [1984]. Calculations based on field measurements of the width of the debris flow, the radius of curvature through the bend, and the down channel slope indicate a velocity of about 9 m s^{-1}, implying a travel time of roughly 2 s to the CB2 weir.

[18] Charcoal samples collected from both the debris-flow headscarp and a soil pit excavated in the upslope hollow constrain the history of previous landsliding at CB2 (Figure 13). A small sample of detrital charcoal collected from the soil/bedrock contact at a depth of 2 m yielded a ^{14}C date of 4070 ± 90 b.p. (CAMS 160). Detrital carbon fragments collected from the base of the colluvial soil exposed in the headscarp of the debris flow yielded a ^{14}C date of 630 ± 110 b.p. (BETA 81760). The different ages for basal charcoal from the channel head and further upslope indicate that either the channel head experienced more recent failure than locations upslope, or the hollow progressively filled from upslope over several thousand years.

4.2. Piezometric Response

[19] Data recorded by automated piezometers document the hydrologic response of CB1 to the debris-flow producing storm. Again, the response of pressure transducers installed in nests with piezometers in both soil and bedrock document substantial response in the fractured bedrock. At some nests, return flow from bedrock influenced the generation of pore pressures in excess of hydrostatic in the colluvial soil. In other nests the near-surface bedrock acted as a drain beneath the colluvial soil. As shown below, piezometric response during the February 1992 storm documents significant spatial variations in shallow bedrock response.

[20] Automated piezometer nests provide a continuous record of piezometric response along the hollow axis at CB1. The discharge response closely tracks the pressure head response at nest 0-1 located immediately upslope of the channel head and the upper weir. The correlation between pressure head at nest 0-1 and discharge through the upper weir for the period from 18 through 22 February (R^2 = 0.77, n = 578) is comparable to relations from previous natural and applied rainfall events [*Montgomery et al.*, 1997]. Piezometer nest 0-1 exhibited infiltrating gradients through the storm and hydrostatic gradients during waning response, but discharge was greater for the same pressure head near the base of the soil during the falling limb of the storm hydrograph, suggesting a local bedrock flow contribution to the CB1 weir during peak discharge and recession.

[21] The deeper automated bedrock nest B4, located downslope and outside of the sealed weir wings, responded to the storm (Figure 14a). While the shallowest bedrock piezometer in this nest (B-4a) did not record saturated conditions during the storm, the deepest piezometer recorded pressure head of roughly 1 meter prior to the storm and increased by about a meter during the storm. During peak response on 20 February, total head in the lower piezometer exceeded the elevation of the upper, dry piezometer, documenting exfiltrating gradients indicative of vertical upward flow from deeper bedrock toward the near-surface fractured bedrock.

[22] Data from bedrock nest B13 and soil nest 5-3, located near the center of the site, recorded the opposite relation (Figure 14b). Here piezometric gradients indicate flow from the fractured bedrock into both the overlying soil and deeper bedrock, as the gradient between the two bedrock piezometers was an infiltrating gradient while simultaneously there was an exfiltrating gradient from the shallow bedrock to the overlying soil. Hence, the fractured bedrock acted like a source that delivered water from upslope to the base of the colluvial soil. Exfiltrating gradients also occurred between the two deepest soil piezometers at this nest during intense rainfall in 1990 [*Montgomery et al.*, 1997].

[23] The combined response of bedrock nest B12 and soil nest 7-6 reveals infiltrating gradients throughout the storm (Figure 14c). Comparable spatial variability in the style of piezometric response along the hollow axis at CB1 occurred during other natural storm events and applied rainfall. In all, these data from the colluvial soil, shallow fractured bedrock, and deeper rock document that the piezometric response of near-surface, fractured bedrock can be quite responsive and is highly variable during natural storm events.

[24] The well at the top of CB1 exhibited a substantial response to the debris flow inducing February 1992 storm (Figure 15). The well began to respond during the storm and continued to rise for several days after the storm, showing a total rise of about 1.5 m in response to the storm. The time lag between peak rainfall and peak well response was again 3 to 4 days, implying a pore pressure-propagation velocity comparable to the mean hydraulic conductivity of the bedrock. In addition, the well level dropped slowly after the

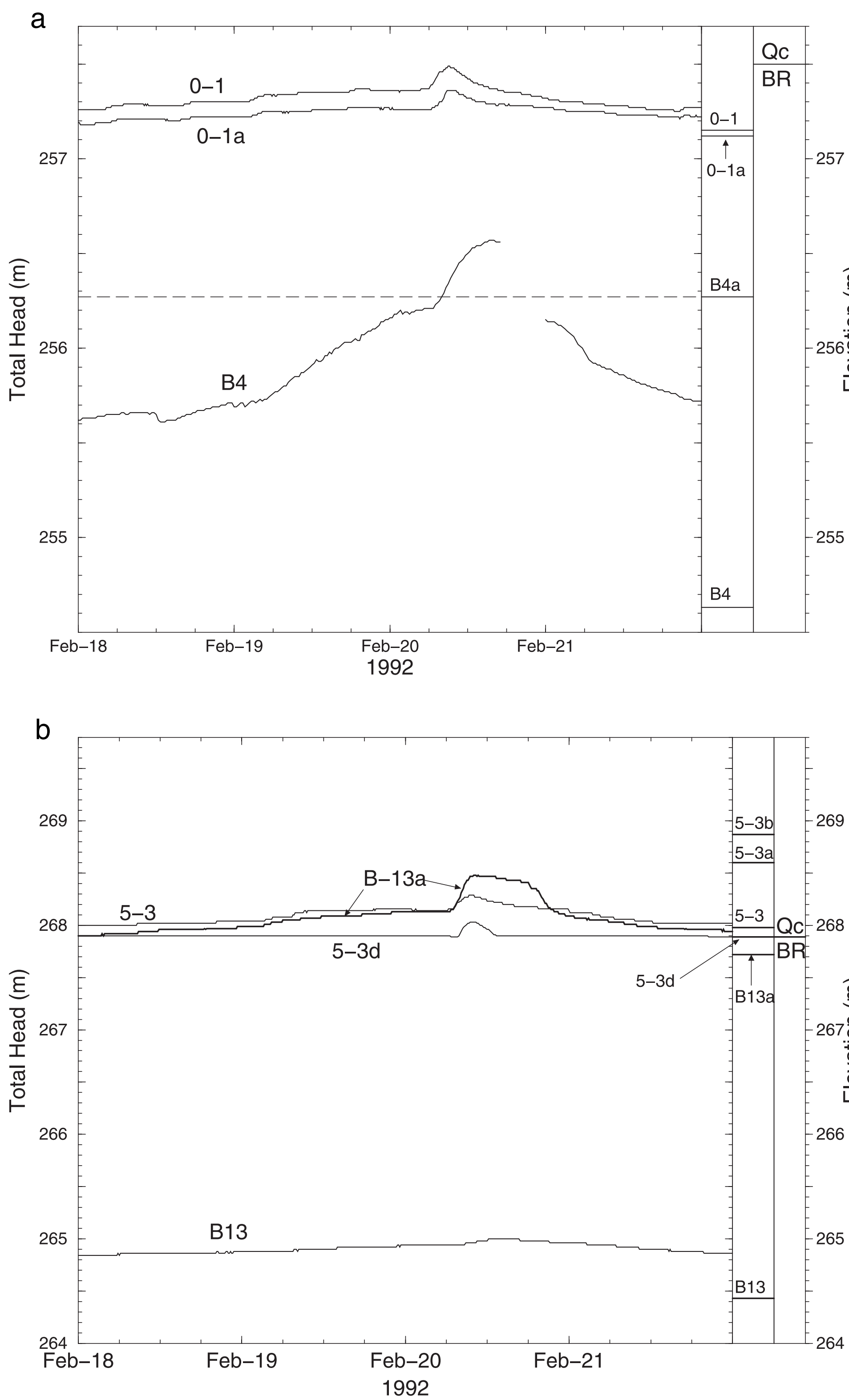

Figure 14. Piezometric response at CB1 for three piezometer nests with pipes installed into near-surface bedrock during the debris flow producing storm in February 1992: (A) soil nest 0-1 and bedrock nest B4. Dashed line for piezometer B-4 indicates no response. (B) soil nest 5-3 and bedrock nest B13; and (C) soil nest 7-6 and bedrock nest B12. Vertical columns on right of figure show elevation of piezometer inlets and the contact between colluvial soil (Qc) and bedrock (BR). Ground surface elevation corresponds to top of each graph.

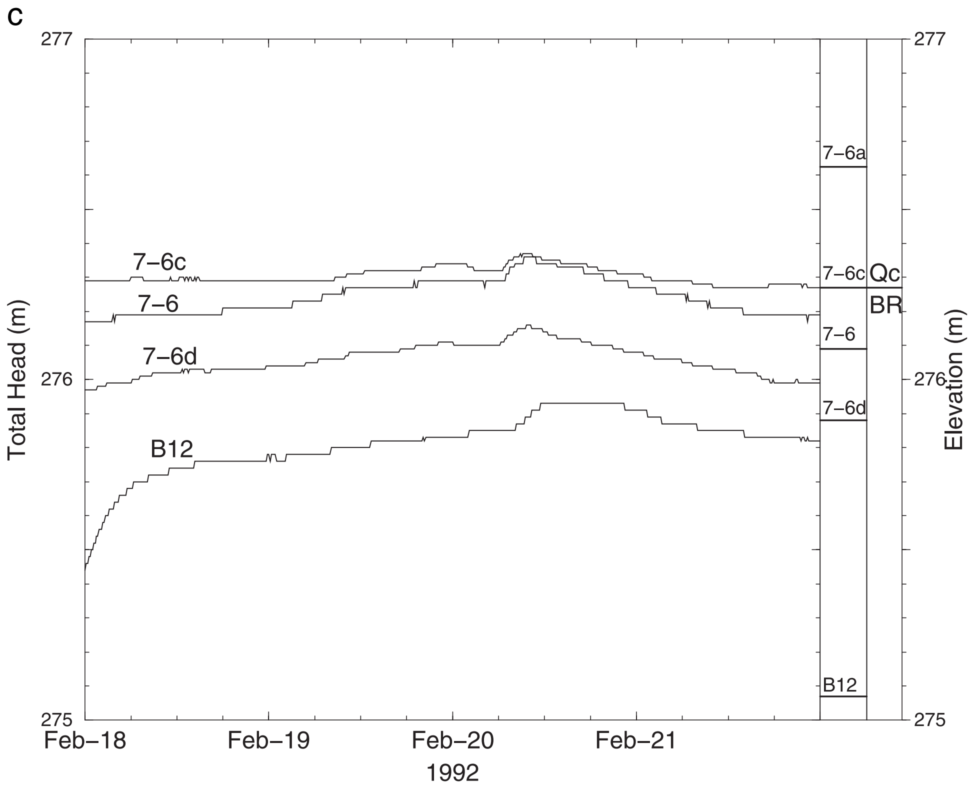

Figure 14. (continued)

storm, indicating a lasting influence of recharge to the shallow groundwater table due to this runoff producing event.

4.3. Pressure Head Propagation

[25] Least squares linear regression of data from CB1 during the February 1992 storm indicates that the time lag between peak rainfall and peak piezometric response is independent of distance upslope from the upper weir (R^2 = 0.02, p = 0.48) but increases with depth below the ground surface (R^2 = 0.42, p < 0.001) (Figure 16). *Torres et al.* [1998] showed that pressure head throughout the colluvial soil rapidly attained values close to zero during the sprin-

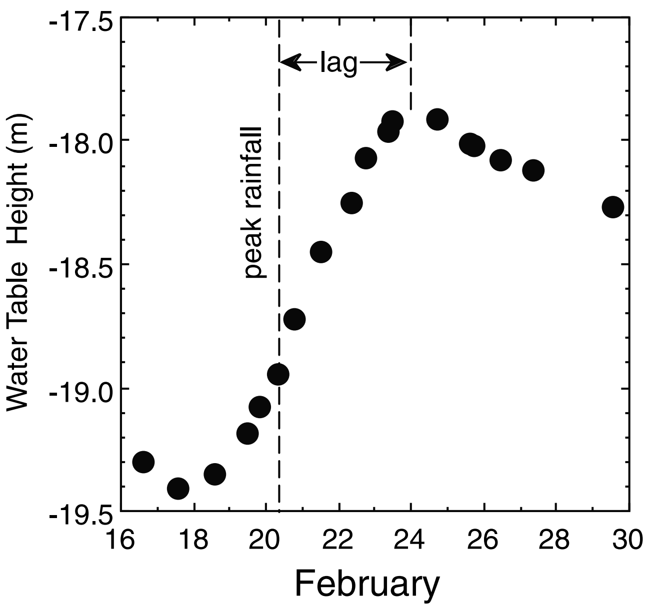

Figure 15. Response of the well located at the top of CB1 to the February 1992 storm, expressed as the height of the water table below the ground surface.

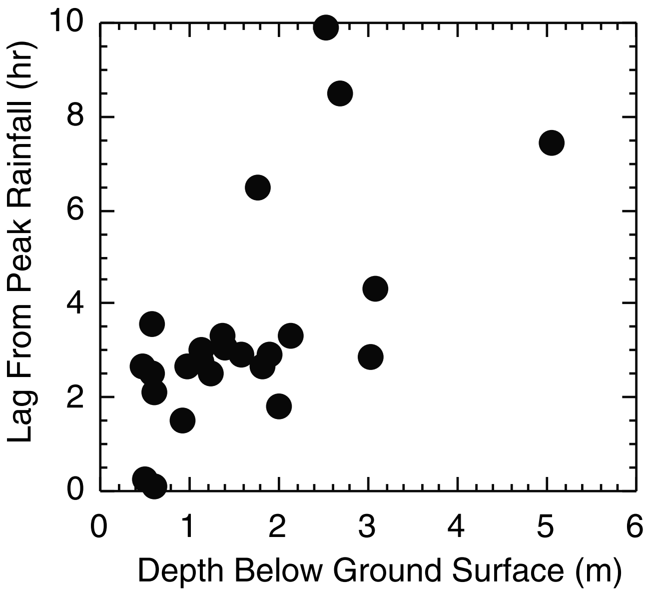

Figure 16. Lag time (hr) between peak rainfall and peak piezometric response for CB1 during the debris flow producing storm in February 1992 versus depth below ground surface, *D* (m). Least squares linear regression yields: $L_p = 1.171 + 1.411\ D$; $R^2 = 0.42$, p < 0.001.

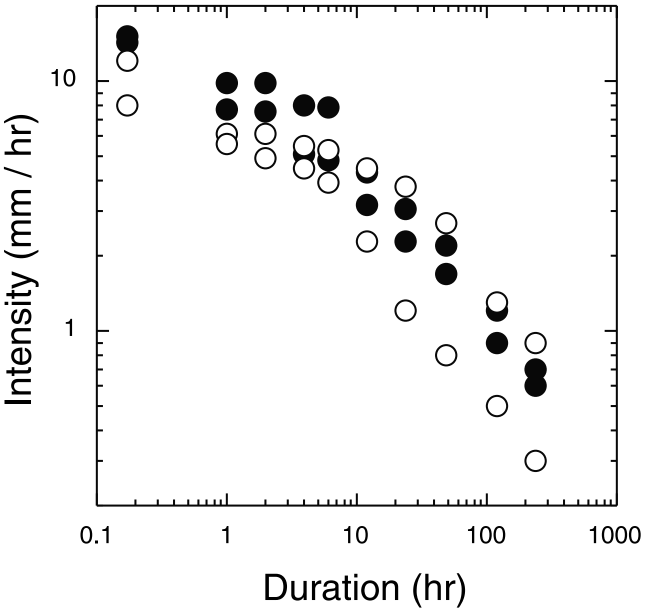

Figure 17. Maximum 10-minute to 10-day rainfall intensity for four 1990 storms; solid circles are for storms during which debris flows occurred along Mettman Ridge (January and April), and open circles are for storms that did not cause debris flows (February and March).

kling experiments, even though the volumetric water content remained far from saturated. Hydraulic conductivity varies greatly in partially saturated soil, and hence linear diffusion models for predicting pressure head response to a pulse of rain do not apply [e.g., *Haneberg*, 1991; *Reid*, 1994; *Baum and Reid*, 1995]. The time lag between peak rainfall and peak piezometric response indicates that the timescale of piezometric response at CB1 varies from <1 to 10 hr.

[26] *Iverson* [2000] used a linear diffusion approach to analyze the timescales pertinent to landslide triggering by rainfall infiltration and found that the quasi-steady groundwater response time given by the minimum time to transmit lateral pore pressures to a point can be approximated by A/D_0, where A is the upslope contributing area (m^2) and D_0 is the hydraulic diffusivity (m^2 t^{-1}) (taken as the product of the average saturated conductivity and soil depth). He also found that the timescale for slope-normal propagation of pore pressures from the ground surface to a depth H is given by H^2/D_0. Iverson proposed using $H = 1$ m, $A = 100$ m^2 and a $D_0 = 10^{-3}$ m^2 s^{-1} to estimate $A/D_0 \approx 1$ day and $H^2/D_0 = 3$ hr for CB1. These values predict rainfall durations longer than 24 hours would not be expected to strongly influence landslide initiation at this site and rainfall intensity over <3 hours duration should most strongly influence landslide initiation. Rainfall intensity and duration data from a series of four storms, two of which triggered landslides along Mettman Ridge in the winter of 1990 [*Montgomery*, 1991], show that those storms with the highest 10 minute to 2 hour rainfall intensity triggered landslides whereas one of the two storms with the greatest intensity for >24 hours duration did not trigger debris flows (Figure 17). Hence, the general timescales predicted by *Iverson* [2000] agree reasonably well with those observed for Mettman Ridge, even though the assumption about near-saturated conditions is violated.

[27] This agreement, however, is very sensitive to the parameter values selected by Iverson for his analysis. Using the actual drainage area of CB1 (860 m^2), a soil depth of 1 m, and the mean soil conductivity of 1×10^{-4} m s^{-1}, yields estimates of $A/D_0 = 100$ days and $H^2/D_0 = 30$ hr CB1. Moreover, as K in the colluvial soil varies from 10^{-3} to 10^{-4} m^2/s and H varies from 0.5 to 2.0 m, then D_0 (calculated as $K \cdot H$) varies locally at CB1 from about 2.5×10^{-5} m^{2}s^{-1} to 4×10^{-3} m^{2}s^{-1}; these values would imply that the range of estimated values for A/D_0 spans 2.5 to 398 days and H^2/D_0 ranges from 1 minute to 2 days across CB1. Hence, the variability in soil depth and hydraulic diffusivity is high enough that the uncertainty on such predictions is greater than an order of magnitude, and essentially spans the entire spectrum of concern for debris flow hazard applications. Nonetheless, such analyses show that the timescale that dominates the pore pressure response of CB1 is that for vertical propagation of pore pressure response from the ground surface to the saturated zone.

5. Seasonal Response

[28] Seasonal records of piezometric response show consistent event-driven response in the fractured bedrock that can approach 1 m during relatively common storms, even in piezometers installed several meters into bedrock. Some response is seen in most of the bedrock piezometers during most storm sequences, but exfiltrating gradients develop only in particular nests during the largest storms. Although our data provide only a fragmentary record of the seasonal response, the depth to the water surface in the well varied by over 7 m in 1992, demonstrating substantial variability in the water depth at the ridge crest. Piezometric records from the top, middle, and bottom of CB1 characterize spatial differences in the seasonal dynamics of near-surface bedrock response.

[29] The seasonal record for the bedrock piezometer nests shows a similar response to storm events throughout the year (Figure 18). Most of the bedrock piezometers have a "base" head level from which the piezometric potential quickly rises and then returns to after storms. In addition, the total head increase is surprisingly similar for a variety of storms. *Wilson and Dietrich* [1987] observed a similar tendency for pressure heads to reach common values in different storms for the case where saturated overland flow drained seepage and prevented greater head development. Similarly at Coos Bay, perhaps, the water exfiltrating from the bedrock is drained by the highly conductive colluvial soil, thereby preventing high heads from developing.

[30] The piezometer nest at the base of the slope (Figure 18a) records development of a perched water table in the colluvial soil, as the middle bedrock piezometer installed immediately below the soil/bedrock contact (not shown) remained dry during the entire year, even though the deepest bedrock piezometer exhibited up to 1.5 m of pressure head response during winter storm events. The piezometric response of soil nest 5-3 and bedrock nest B-13 (Figure 18b) illustrates significant seasonal variation in the coupling of flow in soil and underlying fractured bedrock. During midwinter storms, exfiltrating gradients develop from the shallow bedrock into the overlying soil, whereas

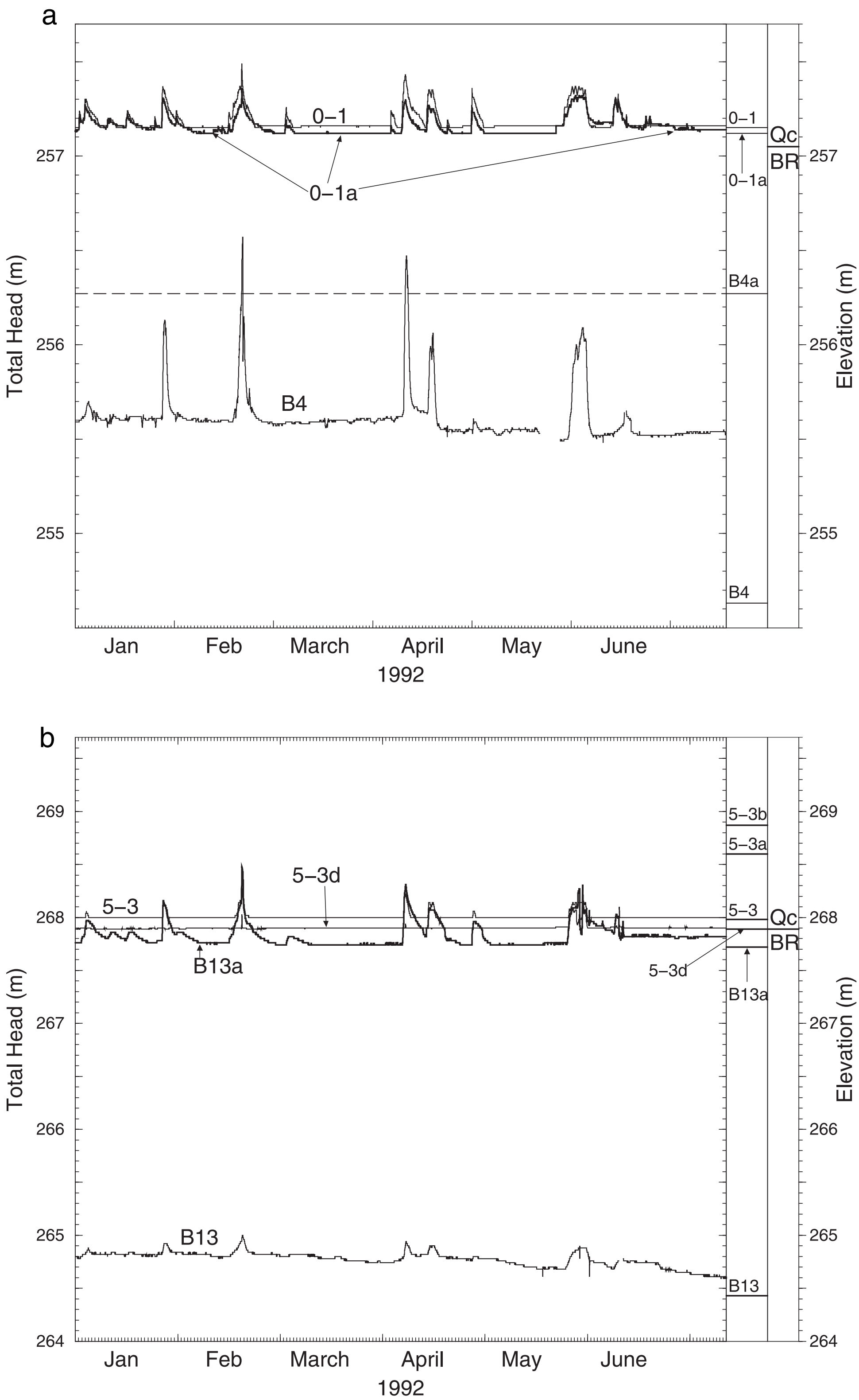

Figure 18. Piezometric response of three piezometer nests with pipes installed into near-surface bedrock during hydrologic year from October 1992 through September 1993: (A) soil nest 0-1 and bedrock nest B4; (B) soil nest 5-3 and bedrock nest B13; and (C) soil nest 7-6 and bedrock nest B12. Vertical columns on right of figure show elevation of piezometer inlets and the contact between colluvial soil (Qc) and bedrock (BR). Ground surface elevation corresponds to top of each graph.

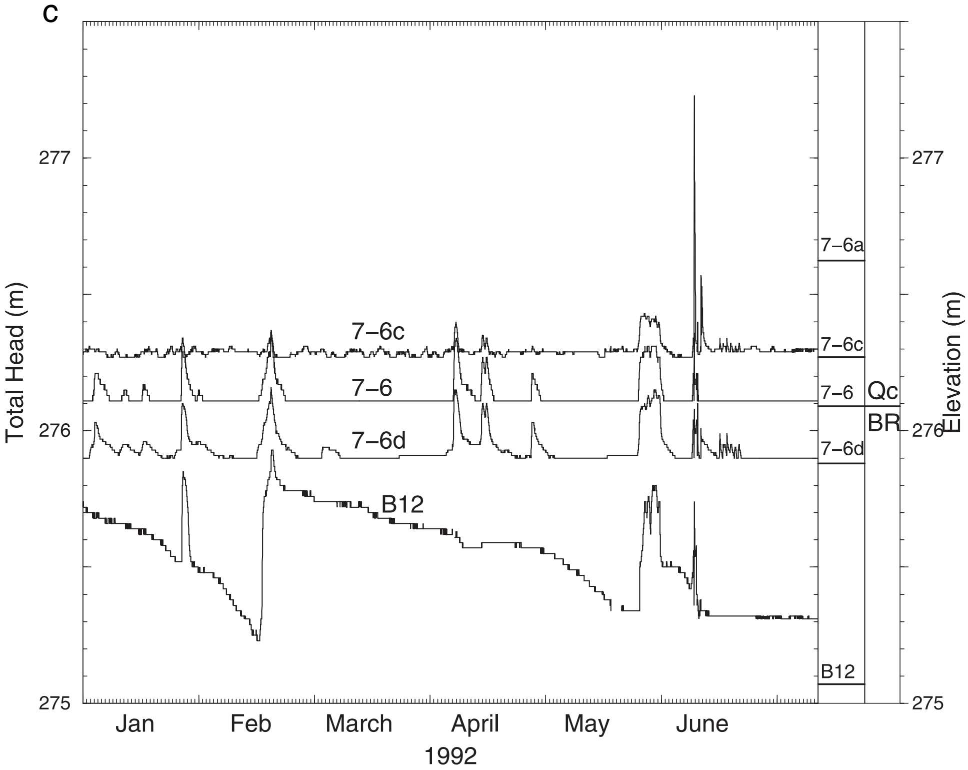

Figure 18. (continued)

the response is primarily infiltrating during the early season. Although the piezometric response of soil nest 7-6 and bedrock nest B12 (Figure 18c) also shows dramatic storm response in the bedrock piezometers, piezometric gradients remain infiltrating. These three piezometer nests exhibit styles of piezometric response that differ from each other but remained consistent through our sprinkling experiments, natural storms, and seasonal variations in rainfall.

6. Discussion

[31] The great variability in saturated hydraulic conductivity, and particularly the lack of any relation to depth within bedrock means that there will be substantial heterogeneity to near surface hydrologic response. This lack of a depth dependence conflicts with the assumptions in TOPMODEL [*Beven and Kirkby*, 1979] and most applications of other models of hillslope hydrology [e.g., *O'Loughlin*, 1986]. Our results indicate that assuming either a simple depth dependent, or spatially constant hydraulic conductivity could mask dynamics with significance for runoff generation and landsliding. If bedrock fractures control pressure head in bedrock, as well as locally in the overlying colluvial soil, and knowledge of the fracture distribution and characteristics is practically impossible to obtain, then use of dynamic hydrologic models to predict the specific locations of shallow landslides may prove no more insightful for hazard assessment than interpretation of simple topographically driven models used to predict zones of high landslide potential.

[32] Our finding that many of the shallower bedrock piezometers show short time delays to peak rainfall demonstrates rapid piezometric response without full soil saturation. Such rapid response reflects a steep soil characteristic curve such that the conductivity increases rapidly as the moisture increases [*Torres et al.*, 1998]. *Anderson et al.* [1997] found that in Experiment 3, the water moved as plug flow at a rate close to the precipitation rate (corrected for porosity) as expected from unsaturated flow theory. Hence, our observations establish that the timescale of piezometric response in shallow bedrock, and the consequent runoff generation by subsurface storm flow, is much faster than the transit time for water moving through the soil. The porosity corrected velocity for propagation of precipitation into the soil (1.65 mm $hr^{-1}/0.5$ = 3.3 mm hr^{-1}) is roughly 1% of the 290 mm hr^{-1} velocity implied by the roughly 7 hours required for piezometric response to travel through the approximately 1 m deep soil and another 1 m into bedrock. This rapid response of the shallow bedrock demonstrates the rapid transmission of pressure waves through unsaturated soil to influence the piezometric response in the underlying fractured rock.

[33] The groundwater table is very high at CB1 because of the low conductivity and negligible storage in the deep, unweathered bedrock beneath the site. This shallow and responsive water table interacts with the steep topography to control the location of the channel head at the base of CB1 and likely influences locations where positive pore pressures develop in the colluvial soil. The position of the onset of streamflow at the base of CB1 remained relatively stationary, whereas the water table in the well at the ridgetop varies by many meters over a year. This variation indicates a potential for interaction between the local perched water table in the colluvial soil and the deeper groundwater table to change through the year as the storage in the intervening material fills. Maximum coupling between the response in near-sur-

face fractured rock and the colluvial soil would occur during storms when antecedent soil moisture is high and the available bedrock storage is low. The seasonal changes in the water table at the ridgetop imply that base flow at the site is not fed by lateral unsaturated flow (as commonly assumed for steep hillslopes) but by slow vertical unsaturated flow and lateral drainage of the near-surface bedrock.

6.1. Role of Near-Surface Fractured Bedrock in Slope Stability

[34] The variable styles of hydrologic interaction between fractured bedrock and colluvial soil apparent in the piezometric response at CB1 show that local variations in the conductivity of the underlying fractured bedrock strongly influence pore pressure generation in the overlying colluvium, as inferred previously by *Pierson* [1977], *Wilson and Dietrich* [1987], and *Montgomery et al.* [1997]. Lateral saturated drainage through near-surface fractured bedrock may lead to locally elevated pressure head that triggers landsliding, but fractured rock also promotes slope stability by accommodating a significant portion of storm runoff, and thereby decreasing saturation in the overlying colluvium. On steep slopes, horizontal exfiltration from the bedrock, as would be expected from either a horizontal fracture daylighting on the slope or from downslope thinning of the hydrologically active zone of near-surface bedrock, is the seepage orientation most conducive to slope failure [*Iverson and Major*, 1986]. The distribution and connectivity of the near-surface bedrock fracture system, which are almost impossible to predict, may effectively determine the specific locations where debris flows initiate. *Pierson* [1983] showed that a blocked macropore would raise the pressure head in the surrounding soil in proportion to the head difference within the macropore. Similarly, the pressure head developed in a sealed fracture is a function of its upslope connectivity. The additional pressure head added by flow exfiltrating from bedrock fractures may contribute to instability along hollow axes where convergence-induced saturation occurs, but elevated pore pressures are difficult to maintain due to the highly conductive soil. Flow exfiltrating from bedrock fractures also could contribute to debris-flow initiation on steep side slopes or locations where soils are thin and partial saturation of the soil profile sufficient to induce instability does not require substantial flow. The location of shallow landsliding in steep terrain therefore appears to be influenced by both topographically controlled flow convergence and spatial variability in the conductivity of near-surface fractured bedrock.

7. Conclusions

[35] The hydrologic response of CB1 shows that shallow bedrock storm flow is an important runoff generation mechanism even in an environment with massive, gently dipping sandstone where one might expect such influences to be minimal. We find it both surprising and interesting that there is seasonal and storm-scale interaction with a deeper bedrock water table on such a steep hillslope. Topographically driven models of runoff generation and shallow landslide hazards are valuable tools for use in landslide hazard assessments and models of landscape evolution, but substantial uncertainty appears inevitable in basin-wide, spatially explicit predictions of the specific timing and location of debris-flow initiation due to the influence of bedrock heterogeneity on the locations of exfiltration gradients, as well as the previously recognized influences of variations in soil properties and thickness [e.g., *Dietrich et al.*, 1995], and in root reinforcement as influenced by vegetation species, age, and health [e.g., *Schmidt et al.*, 2001].

[36] **Acknowledgments.** This project was supported by National Science Foundation grants CMS-9610269 and EAR-8917467, and the Weyerhaeuser Company. Ray Torres, Suzanne Anderson, and Lee MacDonald helped install bedrock piezometers at CB1. Suzanne Anderson, Robert Anderson, and John Buffington provided field assistance immediately after the debris flow at CB2. Tamara Massong, Darryl Granger and Matt Coglon provided field assistance for topographic surveying. Joel VanderKwaak and Keith Loague analyzed the conductivity test data. Jim Clarke and Kate Sullivan provided tactical and logistical support for our Coos Bay studies. We also thank Bill Haneberg for his useful critique of the manuscript.

References

Anderson, S. P., W. E. Dietrich, D. R. Montgomery, R. Torres, M. E. Conrad, and K. Loague, Subsurface flow paths in a steep unchanneled catchment, *Water Resour. Res.*, *33*, 2637–2653, 1997.

Baum, R. L., and M. E. Reid, Geology hydrology, and mechanics of a slow-moving, clay-rich landslide, Honolulu, Hawaii, in *Clay and Shale Slope Instability*, *Geol. Soc. Am. Rev. Eng. Geol.*, vol. 10, edited by W. C. Haneberg and S. A. Anderson, pp. 79–105, Geol. Soc. of Am., Boulder, Colo., 1995.

Beaulieu, J. D., and P. N. Hughes, Environmental geology of Western Coos and Douglas Counties, Oregon, *Oregon Dep. Geol. Min. Ind. Bull.*, *87*, 148 pp., 1975.

Beschta, R. L., Long-term patterns of sediment production following road construction and logging in the Oregon Coast Range, *Water Resour. Res.*, *14*, 1011–1016, 1978.

Beven, K., and M. J. Kirkby, A physically based, variable contributing area model of basin hydrology, *Hydrol. Sci. Bull.*, *24*, 43–69, 1979.

Brown, G. W., and J. T. Krygier, Clear-cut logging and sediment production in the Oregon Coast Range, *Water Resour. Res.*, *7*, 1189–1198, 1971.

Burton, A., and J. C. Bathurst, Physically based modelling of shallow landslide sediment yield at a catchment scale, *Environ. Geol.*, *35*, 89–99, 1998.

Costa, J. E., Physical geomorphology of debris flows, in *Developments and Applications of Geomorphology*, edited by J. E. Costa and P J. Fleisher, pp. 268–317, Springer-Verlag, New York, 1984.

Dietrich, W. E., and T. Dunne, Sediment budget for a small catchment in mountainous terrain, *Z. Geomorphol.*, *29*, 191–206(supplement), 1978.

Dietrich, W. E., C. J. Wilson, and S. L. Reneau, Hollows, colluvium, and landslides in soil-mantled landscapes, in *Hillslope Processes*, edited by A. D. Abrahams, pp. 361–388, Allen and Unwin, Concord, Mass., 1986.

Dietrich, W. E., C. J. Wilson, D. R. Montgomery, and J. McKean, Analysis of erosion thresholds, channel networks and landscape morphology using a digital terrain model, *J. Geol.*, *101*, 259–278, 1993.

Dietrich, W. E., R. Reiss, M.-L. Hsu, and D. R. Montgomery, A process-based model for colluvial soil depth and shallow landsliding using digital elevation data, *Hydrol. Proc.*, *9*, 383–400, 1995.

Dietrich, W. E., D. Bellugi, and R. Real de Asua, Validation of the shallow landslide model, SHALSTAB, for forest management, in *Land Use and Watersheds: Human Influence on Hydrology and Geomorphology in Urban and Forest Areas*, edited by M. S. Wigmosta and S. J. Burges, pp. 195–227, AGU, Washington, D. C., 2001.

Dunne, T., Stochastic aspects of the relations bewteen climate, hydrology and landform evolution, *Trans. Jpn. Geomorphol. Union*, *12*, 1–24, 1991.

Ellen, S. D., S. H. Cannon, and S. L. Reneau, Distribution of debris flows in Marin County, in *Landslides, Floods and Marine Effects of the Storm of January 3–5, 1982, in the San Francisco Bay region, California*, *U.S. Geol. Surv. Prof. Pap. 1434*, edited by S. D. Ellen and G. F. Wieczorek, pp. 113–131, U. S. Gov. Print. Off., Washington, D.C., 1988.

Ellen, S. D., R. K. Mark, S. H. Cannon, and D. L. Knifong, Map of debris-flow hazard in the Honolulu District of Oahu, Hawaii, *U.S. Geol. Surv. Open-File Rep. 93-213*, 25 pp., U. S. Gov. Print. Off., Washington D.C., 1993.

Everett, A. G., Secondary permeability as a possible factor in the origin of debris avalanches associated with heavy rainfall, *J. Hydrol.*, *43*, 347–354, 1979.

Fredriksen, R. L., Erosion and sedimentation following road construction and timber harvest on unstable soils in three small western Oregon watersheds, *Res. Pap. PNW-104*, 15 pp., U.S. Dep. of Agric., For. Serv., Portland, Oreg., 1970.

Haneberg, W. C., Pore pressure diffusion and the hydrologic response of nearly saturated, thin landslide deposits to rainfall, *J. Geol.*, *99*, 886–892, 1991.

Harr, R. D., Water flux in soil and subsoil on a steep forested slope, *J. Hydrol.*, *33*, 37–58, 1977.

Harr, R. D., and C. S. Yee, *Soil and Hydrologic Factors Affecting the Stability of Natural Slopes in the Oregon Coast Range*, *WRRI-33*, 204 pp., Water Resour. Res. Inst., Oreg. State Univ., Corvallis, 1975.

Heimsath, A. M., W. E. Dietrich, K. Nishiizumi, and R. C. Finkel, Stochastic processes of soil production and transport: Erosion rates, topographic variation, and cosmogenic nuclides in the Oregon Coast Range, *Earth Surf. Processes Landforms*, *26*, 531–552, 2001.

Hvorslev, M. J., *Time Lag and Soil Permeability in Groundwater Observations*, *Bull. 36*, 50 pp., U.S. Army Corps of Eng. Waterw. Exp. Stn., Vicksburg, Miss., 1951.

Iverson, R. M., Landslide triggering by rain infiltration, *Water Resour. Res.*, *36*, 1897–1910, 2000.

Iverson, R. M., and J. J. Major, Ground-water seepage vectors and the potential for hillslope failure and debris flow mobilization, *Water Resour. Res.*, *22*, 1543–1548, 1986.

Iverson, R. M., and J. J. Major, Rainfall, ground-water flow, and seasonal movement at Minor Creek landslide, northwestern California: Physical interpretation of empirical relations, *Geol. Soc. Am. Bull.*, *99*, 579–594, 1987.

Mathewson, C. C., J. R. Keaton, and P. M. Santi, Role of bedrock ground water in the initiation of debris flows and sustained post-flow stream discharge, *Bull. Assoc. Eng. Geol.*, *27*, 73–83, 1990.

May, C. L., Debris flow characteristics associated with forest practices in the central Oregon Coast Range, M.S. thesis, 121 pp., Oreg. State Univ., Corvallis, 1998.

Montgomery, D. R., Channel initiation and landscape evolution, Ph.D. dissertation, 421 pp., Univ. of Calif., Berkeley, 1991.

Montgomery, D. R., and W. E. Dietrich, Where do channels begin?, *Nature*, *336*, 232–234, 1988.

Montgomery, D. R., and W. E. Dietrich, A physically-based model for the topographic control on shallow landsliding, *Water Resour. Res.*, *30*, 1153–1171, 1994.

Montgomery, D. R., and W. E. Dietrich, Runoff generation in a steep, soil-mantled landscape, *Water Resour. Res.*, *38*(9), 1168, doi:10.1029/2001WR000822, 2002.

Montgomery, D. R., W. E. Dietrich, R. Torres, S. P. Anderson, J. T. Heffner, and K. Loague, Piezometric response of a steep unchanneled valley to natural and applied rainfall, *Water Resour. Res.*, *33*, 91–109, 1997.

Montgomery, D. R., K. Sullivan, and H. M. Greenberg, Regional test of a model for shallow landsliding, *Hydrol. Proc.*, *12*, 943–955, 1998.

Montgomery, D. R., K. M. Schmidt, H. Greenberg, and W. E. Dietrich, Forest clearing and regional landsliding, *Geology*, *28*, 311–314, 2000.

Montgomery, D. R., H. M. Greenberg, W. T. Laprade, and W. D. Nasham, Sliding in Seattle: Test of a model of shallow landsliding potential in an urban environment, in *Land Use and Watersheds: Human Influence on Hydrology and Geomorphology in Urban and Forest Areas*, edited by M. S. Wigmosta and S. J. Burges, pp. 59–73, AGU, Washington, D. C., 2001.

Okimura, T., and R. Ichikawa, A prediction method for surface failures by movements of infiltrated water in a surface soil layer, *Nat. Disaster Sci.*, *7*, 41–51, 1985.

Okimura, T., and M. Nakagawa, A method for predicting surface mountain slope failure with a digital landform model, *Shin-Sabo*, *41*, 48–56, 1988.

O'Loughlin, E. M., Prediction of surface saturation zones in natural catchments by topographic analysis, *Water Resour. Res.*, *22*, 794–804, 1986.

Pierson, T. C., Factors controlling debris-flow initiation on forested hillslopes in the Oregon Coast Range, Ph.D. dissertation, 166 pp., Univ. of Wash., Seattle, 1977.

Pierson, T. C., Piezometric response to rainstorms in forested hillslope drainage depressions, *J. Hydrol. N. Z.*, *19*, 1–10, 1980.

Pierson, T. C., Soil pipes and slope stability, *Q. J. Eng. Geol.*, *16*, 1–11, 1983.

Reid, M. E., A pore-pressure diffusion model for estimating landslide-inducing rainfall, *J. Geol.*, *102*, 709–717, 1994.

Reneau, S. L., and W. E. Dietrich, Size and location of colluvial landslides in a steep forested landscape, in *Erosion and Sedimentation in the Pacific Rim*, *Int. Assoc. Hydrol. Sci. Publ.*, vol. 165, edited by R. L. Beschta et al., pp. 39–49, Int. Assoc. of Hydrol. Sci., Wallingford, U.K., 1987.

Schmidt, K. M., Root strength, colluvial soil depth, and colluvial transport on landslide-prone hillslopes, Ph.D. dissertation, Univ. of Wash., Seattle, 1999.

Schmidt, K. M., J. R. Roering, J. D. Stock, W. E. Dietrich, D. R. Montgomery, and T. Schaub, Root cohesion variability and shallow landslide susceptibility in the Oregon Coast Range, *Can. Geotech. J.*, *38*, 995–1024, 2001.

Schroeder, W. L., and J. V. Alto, Soil properties for slope stability analysis; Oregon and Washington coastal mountains, *Forest Sci.*, *29*, 823–833, 1983.

Torres, R., W. E. Dietrich, D. R. Montgomery, S. P. Anderson, and K. Loague, Unsaturated zone processes and the hydrologic response of a steep unchanneled catchment, *Water Resour. Res.*, *34*, 1865–1879, 1998.

Wilson, C. J., and W. E. Dietrich, The contribution of bedrock groundwater flow to storm runoff and high pore pressure development in hollows, in *Erosion and Sedimentation in the Pacific Rim*, *IAHS Publ.*, vol. 165, edited by R. L. Beschta et al., pp. 49–60, Int. Assoc. of Hydrol Sci., Wallingford, U.K., 1987.

Wu, W., and R. C. Sidle, A distributed slope stability model for steep forested basins, *Water Resour. Res.*, *31*, 2097–2110, 1995.

W. E. Dietrich, Department of Earth and Planetary Science, University of California, Berkeley, CA 94720, USA.

J. T. Heffner, Environmental Research, Weyerhaeuser Company, 505 North Pearl Street, Centralia, WA 98531, USA.

D. R. Montgomery, Department of Earth and Space Sciences, University of Washington, Seattle, WA 98195, USA. (dave@geology.washington.edu)